

Cytokine-secreting follicular T cells shape the antibody repertoire

R. Lee Reinhardt¹, Hong-Erh Liang¹, and Richard M. Locksley¹

¹Howard Hughes Medical Institute and Departments of Medicine and Microbiology & Immunology, University of California San Francisco, San Francisco, CA 94143

Abstract

High-affinity antibodies are critical for host protection and underlie successful vaccines. Generation of such antibodies requires T cell-dependent help, which mediates germinal center (GC) reactions where mutation and selection of B cells occurs. Using an interleukin 4 (IL-4)-reporter system, we show that follicular CD4₊ T (T_{FH}) cells comprised essentially all of the cytokine-secreting T cells in lymph nodes and were functionally distinct from T cells secreting the same cytokine in peripheral tissues. T_{FH} cells with different cytokine profiles could be isolated as conjugates with B cells undergoing cytokine-specific immunoglobulin class-switching with evidence of somatic hypermutation. These findings support a model wherein B cells compete for cytokines produced by T_{FH} cells that shape the affinity and isotype of the antibody response.

Keywords

follicular helper T cells; cytokines; germinal center; Th1/Th2 cells; B cell selection

A critical component of protective immunity is the generation of long-lived memory B cells and plasma cells, which produce high-affinity antibodies against foreign antigens. The classic model of affinity maturation postulates that germinal center (GC) B cells in the GC dark zone, termed centroblasts, undergo extensive proliferation and somatic hypermutation before entering the GC light zone where they differentiate into centrocytes. Selection occurs when high-affinity centrocytes in the light zone of the GC are selected by follicular dendritic cells (FDCs) presenting antigen in the form of immune complexes^{1–3}. Although it is clear that affinity for antigen plays a critical role in selection, evidence that mice that lack immune complexes or with deficits in B cell receptor signaling can form normal GCs suggests that cells other than FDCs also play a role in B cell selection^{4–7}. These studies raise the question of whether, in addition to competition for antigen, the mechanism for the selection of high-affinity clones and the induction of isotype-switching may also be influenced by the ability of GC B cells to compete for help from rare GC T cells. Indeed, theoretical models and imaging experiments raise the possibility that T cell help could

Users may view, print, copy, and download text and data-mine the content in such documents, for the purposes of academic research, subject always to the full Conditions of use:http://www.nature.com/authors/editorial_policies/license.html#terms

Correspondence should be addressed to R. M. L., (locksley@medicine.ucsf.edu).

Author Information

The authors declare no competing financial interests.

represent the most efficient mechanism for achieving selection of high-affinity GC B cells^{8–10}.

CD4⁺ T cells in the follicles, termed T follicular helper cells (T_{FH}), are thought to play an important role in these processes¹¹. Furthermore, these T cells serve as an important reservoir of memory cells in secondary responses to antigen¹². However, how these rare T cells interact with antigen-specific B cells to mount a primary T cell-dependent immune response is not defined. Clearly, T cell help in the form of cognate B–T interactions and CD40 ligation is critical for GC formation, function and optimal antibody response^{13, 14}. Similarly, cytokines, such as interleukin 4 (IL-4; <http://www.signaling-gateway.org/molecule/query?afcsid=A001262>) and interferon- γ (IFN- γ ; <http://www.signaling-gateway.org/molecule/query?afcsid=A001238>), from CD4⁺ T cells are key mediators regulating antibody isotypes by B cells and represent another such possibility. However, previous studies suggest that T_{FH} cells do not express these cytokines and thus it remains unknown whether these cytokines act locally or through some bystander mechanism to help B cells in the GC^{15–17}. Using histochemical and flow cytometric methods to follow the kinetics of IL-4 production by lymphoid T cells during physiologic immune responses, we observed tight spatiotemporal regulation of IL-4 competence and IL-4 secretion, with the latter restricted to T_{FH} cells in the B cell follicles and GCs. Furthermore, directed cytokine secretion by T_{FH} cells in conjugates with GC B cells regulated the size, isotype and affinity of antibodies, showing that cytokines implicated in the function of canonical T_H effector subsets were also critical in mediating the functions of T_{FH} cells.

RESULTS

IL-4 secretion is restricted to T_{FH} cells

To test the role of cytokines in B cell help, we monitored IL-4 production using cytokine-reporter mice, designated 4get \times KN2, that facilitate the sensitive detection of IL-4 competence and secretion by individual cells *in vivo*¹⁸. Cells from the 4get \times KN2 mice express green fluorescent protein (GFP) downstream from an internal ribosomal entry site (IRES) inserted at the 3' end of the *il4* gene (4get), thus identifying cells with an actively transcribed locus, and, on the other allele, a human CD2 (huCD2) marker introduced at the *il4* start site (KN2), identifying cells actively producing IL-4¹⁸. Thus, we can follow activation of the locus by monitoring GFP and recent secretion of IL-4 protein by detecting surface huCD2 on single cells without the need for secondary stimulation.

We first infected BALB/c 4get \times KN2 mice with *Leishmania major* to assess the course of IL-4 competence and secretion in lymph nodes draining the site of parasite inoculation. Despite the similar kinetics for GFP and huCD2 expression on CD4⁺ T cells, immunohistochemistry revealed that IL-4 secretion, as assessed by huCD2 expression, was spatially restricted to distinct regions of the lymph node (Fig. 1; Supplementary Fig. 1 online). GFP expression appeared in the lymph node paracortex near the T cell-B cell border on day 4 post-infection, indicating that T cell differentiation and cytokine competence initially occurs in the T cell zones (Fig. 1a; Supplementary Fig. 1c). By day 6, a small but significant number of these GFP⁺ cells began to appear in the B cell follicles. In contrast, huCD2 expression was restricted primarily to the B cell follicles and GCs throughout

infection (Fig. 1a, Supplementary Fig. 1c). By day 10, many of the IL-4-producing cells were clustered in or around GCs, and by day 21, IL-4-secreting cells resided almost exclusively in GCs (Fig. 1a, Supplementary Fig. 1d). Although concentrated mainly in the light zones on day 14, substantial numbers of IL-4-secreting cells resided in the dark zones at later time points (Fig. 1b). We verified this restricted pattern of IL-4 competence and secretion in lymph nodes after adoptive transfer of ovalbumin (OVA)-specific DO11.10 CD4⁺ T cells (Supplementary Fig. 2 online). Thus, although CD4⁺ T cell proliferation and T_H2 differentiation, as marked by IL-4 expression (GFP), first occurred in the T cell area, the discharge of T_H2 cytokines, as marked by IL-4 secretion (huCD2), was restricted to GFP⁺ cells in the B cell follicles and later in the GCs.

IL-4-secreting T_{FH} cells are distinct from T_H2 cells

The localization of IL-4-expressing lymph node T cells suggested that these cells might indeed be T_{FH} cells, which are specialized for B cell help¹¹. CXCR5, a chemokine receptor involved in the migration of B and T cells into follicles, is expressed by T_{FH} cells^{11, 19}. After infection with *L. major*, a large percentage of the GFP⁺ (IL-4-competent) CD4 T cells increased expression of CXCR5 (Fig. 2a). Furthermore, essentially all huCD2-expressing (IL-4-secreting) CD4⁺ T cells expressed CXCR5 demonstrating that IL-4-producing T cells were capable of entering B cell follicles. The IL-4-expressing CD4⁺ T cells also co-expressed high amounts of inducible costimulator of cytokine secretion (ICOS) (Fig. 2b), another marker expressed by T_{FH} cells¹⁹. Although *in situ* analysis revealed that ICOS was expressed throughout the lymph node during infection (Fig. 2c), co-expression of huCD2 and ICOS first occurred in the parafollicular region at day 6 post-infection, a time and location where antibody secreting-cells make low-affinity antibodies, but by day 14, co-expression of ICOS and IL-4 was restricted primarily to the B cell follicles and more specifically to the GCs. Thus, cytokine-expressing CD4⁺ T cells that developed in response to infection display surface molecules important for movement into B cell follicles and for interacting with B cells in driving GC formation.

ICOS:ICOS-L interactions are required for GC formation and optimal antibody production, but are not needed for T_H2 effector cell differentiation, tissue migration or for eosinophil recruitment to sites of infection^{20–22}. Because ICOS is a critical regulator of T_{FH} cell generation and function, we assessed the effects of ICOS:ICOS-L blockade on the appearance of IL-4-expressing lymph node T cells by treating 4get × KN2 mice with anti-ICOS-L19. Consistent with descriptions using ICOS-deficient mice, anti-ICOS-L-treated mice exhibited reduced GC formation based on the absence of the GC marker peanut agglutinin (PNA) and the GC light zone FDC marker, CD23 (Fig. 3a,b). Blocking ICOS-L also led to a substantial reduction in the number of IL-4-secreting cells, as assessed by huCD2 expression, in the B cell follicles (Fig. 3a–c). ICOS blockade after immunization with protein antigen in alum also led to a reduction in CD95⁺GL7⁺ GC B cells, and the percentages and numbers of IL-4-secreting cells were reduced despite little change in numbers of overall IL-4-competent T_H2 cells as assessed by the GFP marker (Fig. 3c; data not shown). These and the prior results indicate that ICOS-L was not required for T_H2 differentiation but was required for the appearance of cytokine-secreting lymph node T cells, consistent with their identification as *bona fide* T_{FH} cells.

To investigate the generality of IL-4 production by T_{FH} cells during an active T_{H2}-associated immune response, we infected mice with *Nippostrongylus brasiliensis*, a helminth that induces a strong IL-4-dominated host response²³. As compared to lung IL-4-producing T_{H2} cells, IL-4-producing T cells from lymph nodes exhibited higher expression of CXCR5, Slam-associated protein (SAP), the transcription factor BCL-6 and IL-21, and relatively lower expression of sphingosine 1-phosphate receptor-1 (S1P1, a receptor required for lymphocyte egress), consistent with their identification as T_{FH} cells; both subsets expressed IL-4 (Fig. 4a) ¹⁹. To confirm the T_{FH} phenotype, we isolated GFP⁺ cells from *N. brasiliensis*-infected tissues and found that the GFP⁺ cells from the lung produced significantly less IL-21 after activation than did the GFP⁺ cells from the draining lymph node (Fig. 4b).

The differences in IL-21 production suggested that IL-4-producing T_{FH} cells perform different immune functions as compared to canonical nonlymphoid T_{H2} cells. To test this we isolated huCD2⁺CD4⁺ T cells from the lungs or lymph nodes of 4get × KN2 mice infected 10 days previously with *N. brasiliensis*. Cells were adoptively transferred to combined IL-4- and IL-13- deficient mice and the recipient mice were infected with *N. brasiliensis*. Eosinophil recruitment to the lung, which is highly dependent on T_{H2} cells²⁴, was assayed on day 10. The numbers of eosinophils were over 3-fold higher in tissues of mice that received huCD2⁺ cells from the lung as compared to mice that received huCD2⁺ cells from lymph nodes (Fig. 4c). Taken together, these sets of experiments show that IL-4-producing T cells in the lymph nodes were phenotypically and functionally distinct from peripheral T_{H2} cells, and had the canonical characteristics of T_{FH} cells.

T_{FH}-B cell conjugates are sites of T cell help

The unexpected predominance of IL-4 secretion in and around the follicles and the germinal centers led us to hypothesize that competition among GC B cells for rare cytokine-producing GC T cells may underlie antibody isotype class switching and possibly affinity maturation. Among IL-4-producing T_{FH} cells, a small fraction of GFP⁺ or huCD2⁺ cells co-expressed the B cell marker CD19, suggesting that these may represent stable B–T cell conjugates (Fig. 5a; Supplementary Fig. 3 online) ^{9, 25}. Corroborating further their identification as B–T conjugates, GFP⁺ cells that expressed both T and B cell markers were twice the size of the single cells (Fig. 5b). Although isolated GC B cells can form conjugates with T cells *in vitro* and real-time studies have imaged B–T conjugates *in vivo*, no physiological relevance has been established for these conjugates^{25, 26}. To confirm this relevance *in vivo*, we infected mice with *L. major* and isolated B–T conjugates after 3 weeks. As compared to non-IL-4-expressing conjugates, the IL-4-expressing conjugates were greatly enriched for expression of germinal center markers, consistent with localization of cytokine expression to regions of active T cell help (Supplementary Fig. 4 online). B–T conjugates represent a rare population (0.2 to 1% of total lymphocytes) in the lymph node during the course of infection (Fig. 5c; data not shown). Furthermore, IL-4-secreting (huCD2⁺, GFP⁺) and IL-4-competent (huCD2⁻, GFP⁺) conjugates represent only 1 to 3% of total conjugates, respectively (Fig. 5a,c). Indeed, all CD4⁺B220⁺ cells that expressed GFP co-expressed the TCR marker CD3 and represented B–T conjugates (Fig. 5c). To analyze stable conjugates, the small percentage of GFP⁺ or huCD2⁺ cells that co-expressed the T and B cell markers CD4 and

B220 were sorted to high purity and then treated with EDTA to dissociate cell-cell contacts. The resulting single cells segregated into approximately equal numbers of CD4 and B220 single-positive populations, consistent with their original purification as B–T conjugates (Fig. 5d,e). Importantly, all of the GFP⁺ or huCD2⁺ cells were identified as CD4⁺ T cells rather than B cells, consistent with IL-4 production by T_{FH} cells and not by B cells.

To test the role of IL-4 in T cell help, we sorted the B–T cell conjugates from the draining lymph nodes of 4get × KN2 reporter mice infected with *L. major* 14 days previously and used semi-quantitative RT-PCR to assess the expression of activation-induced cytidine deaminase (AID), an enzyme required for somatic hypermutation and isotype class switching and largely confined to GC B cells^{27, 28}. Using this method, GFP⁺huCD2⁺ conjugates expressed more AID than huCD2⁻ conjugates, indicating that B cells in contact with IL-4-producing T cells were enriched for the machinery necessary to induce affinity maturation and isotype class switching (Fig. 5f). Further, B cells conjugated to GFP⁺huCD2⁺ T cells expressed more IgG1 post-switch and germline transcripts than did B cells in GFP⁺huCD2⁻ or GFP⁻huCD2⁻ conjugates, consistent with a role for localized cytokine secretion in IgG1 class switching (Fig. 5f; data not shown).

To assess a more global role for cytokine production by T_{FH} cells in conjugation with GC cells, we used BALB/c mice containing the IL-4-huCD2 replacement marker KN2 on one *il4* allele and an endogenous *ifng* allele altered to express yellow fluorescent protein (YFP) downstream of an IRES element inserted 3' of the endogenous *ifng* gene. We infected these dual reporter mice with *L. major*, which induces both IL-4 and IFN- γ expression in CD4⁺ T cells after infection²⁹, and used immunohistochemistry to assess the capacity of the IFN- γ -expressing cells to enter GCs. Although greater numbers of IL-4-expressing huCD2⁺ cells were present in GCs, as expected after this infection, IFN- γ -expressing cells were readily detected as YFP⁺, often in the same GCs (Fig. 5g). B–T conjugates with IL-4-expressing cells contained IgG1-switched and germline transcripts, whereas the B–T conjugates with IFN- γ -producing cells contained IgG2a-switched and germline transcripts, providing direct evidence that specific cytokine production by T_{FH} cells regulates isotype class switching in conjugated B cells (Fig. 5h).

The elevated amounts of AID in cytokine-expressing B–T conjugates confirms that T cell help is important in somatic hypermutation (SHM) and affinity maturation. To address SHM among B–T conjugates, we utilized the well-defined (4-hydroxy-3-nitrophenyl)acetyl (NP)-alum immunization model to assess the primary immune response to NP in C57BL/6 mice^{30, 31}. The majority of B cells selected during a primary response to proteins conjugated to this hapten preferentially utilize a common V_H186.2 element to assemble their immunoglobulin heavy chains. Using primers specific for the rearranged V_H186.2 heavy chain (or for very closely related V_H elements), we analyzed somatic mutation in antigen-specific B cells by quantifying the numbers of mutations relative to the germline V_H186.2 sequences in purified (non-conjugated) NP-specific B cells as compared to those in the purified B–T conjugates as they accumulated during the immune response (Supplementary Fig.5 online)³⁰. After sorting to high purity, we compared the rate of mutations in the V_H186.2 heavy chain gene segment (mutation in the presence of antigen selection) with the rate of mutations in the intron between the J_H3 and J_H4 elements (mutation insensitive to

selection) as a control. Although the J_H4 intronic region had similar levels of nucleotide mutations between the GFP⁺ B–T conjugates and the NP-specific B cells at day 14 after immunization, the sequences from the B cells in the conjugates were enriched for non-canonical clones and had a 2.7-fold greater mutation rate in the V_H186.2 heavy chain region, consistent with a selection process occurring among the conjugated B cells that held true throughout the response (Fig. 6a,b; Supplementary Fig.5 and Fig.6 online)^{32, 33}. By day 14, 56% of the conjugates had greater than 10 nucleotide mutations within the V-region-containing framework regions (FW) 1–3 and complementarity determining regions (CDR) 1 and 2 as compared to only 6.8% of the NP⁺ B cells. The great majority of these mutations led to amino acid replacements that were localized to the CDRs rather than the FW regions further suggesting that B cells in conjugates were undergoing positive selection (Fig. 6c; Supplemental Fig. 7).

IL-4 is required for IgG1 affinity maturation

To elucidate further the function of IL-4 secretion by T_{FH} cells in GC function, we compared antibody production in heterozygous KN2/+ (IL-4 heterozygous) and homozygous KN2/KN2 (IL-4-deficient as human CD2 replaces *il4* on both alleles) mice ^{34–36}. We observed that KN2/+ and KN2/KN2 mice had similar numbers of huCD2⁺ CD4⁺ T cells and GC B cells in the lymph node throughout the immune response confirming that IL-4 was not required for GC formation (Fig. 7a,b). Although IL-4-deficient mice had a similar percentage of antigen-experienced, antigen-specific IgD[–], CD38[–] B cells as did IL-4-sufficient animals, IgG1 antibody-secreting B cells in the draining lymph nodes and bone marrow, as well as serum IgG1, were reduced significantly in the absence of IL-4 (Fig. 7c; Supplementary Fig. 8a online). IgG1-switched B cells arising in the presence of IL-4 were almost exclusively GC B cells, as indicated by their high expression of GL7 (Supplementary Fig. 8b). Of note, IL-4-deficient mice also showed substantially impaired affinity maturation within the IgG1-expressing B cell pool but not within the IgG2a-expressing pool, indicating a previously unknown role for IL-4-producing T_{FH} cells in the maturation and/or selection of high-affinity antibodies of this isotype (Fig. 7d; Supplementary Fig. 9 online).

To ascertain whether IL-4-producing T_{FH} cells are sufficient for IgG1 selection and affinity maturation, we isolated GFP⁺ or GFP⁺huCD2⁺ CD4⁺ T cells from OVA-NP(15)-immunized dual reporter mice and transferred them into naïve combined IL-4 and IL-13-deficient animals, thereby creating a model where IL-4 was only produced by the transferred T_{FH} cells that had committed to IL-4 production. Recipient mice were then challenged with OVA-NP(15) and assayed on day 14 for the ability of the transferred T cells to help B cells. The combined IL-4 and 13-deficient mice that received GFP⁺ or huCD2⁺ CD4⁺ T cells generated significantly more NP-specific IgG1 antibody-secreting cells, IgG1-switched GC B cells and higher serum IgG1 titers than did non-transferred controls (Fig. 7e; Supplementary Fig. 10 online). Moreover, the IgG1 produced by these mice had higher affinity for antigen, indicating that NP-specific B cells had undergone affinity maturation even at this early time point (Fig. 7f). Thus, these data demonstrate that T_{FH} cells play an indispensable role for the optimal maturation and selection of high-affinity IgG1 antibodies through the secretion of IL-4, thus defining specific cytokine secretion by T_{FH} cells as a key

component of T cell help not only for isotype switching, but also for qualitative changes in the antibody response.

DISCUSSION

Although the requirements for antigen and T cell help for B cell selection have been long established^{1–3, 7}, the precise role for the canonical T_H effector cytokines in the GC reaction process remains controversial¹⁹. IL-21 and ICOS are critical for T_{FH} development, and a role for T_{FH} cells in antibody production is clearly evident^{16, 17}. However, studies suggest that the effects of IL-21 on antibody production are due to indirect effects on the generation of T_{FH} cells rather than to direct effects on B cells. Thus, the precise role of T_{FH}-derived effector cytokines in providing B cell help remained unresolved. Earlier studies suggested that T_{FH} represent a distinct T-helper subset due to their lack of expression of canonical transcription factors required for the elaboration of various subsets of T_H2 (IL-4), T_H1 (IFN- γ) and T_H17 (IL-17) cytokines^{15, 17}. Hence, it remains an open question as to how cytokines, such as IFN- γ and IL-4, which are known to be critical for antibody production, could regulate B cell responses *in vivo*. The unexpected observation that essentially all of the IL-4-secreting cells in the lymph nodes were T_{FH} cells argues that these cytokines act directly in mediating help for B cells in the follicles and GCs. Indeed, our analysis of B–T cell conjugates supports a direct role for IL-4 and IFN- γ in defining the size, class and affinity of antibodies generated during physiologic immune responses *in vivo*. Because T cells residing in the follicles represent only a small subset of the CXCR5⁺, ICOS⁺ T cells after infection or immunization, our ability to detect cytokine secretion *in situ* allowed us to analyze T_{FH} cells based on location and function rather than by expression of cell surface markers, which are expressed not only by T_{FH} cells but also by the majority of activated T cells in lymph nodes.

The relationship between T_{FH} cells and canonical T_H2 cells has been controversial¹⁹. We show that follicular IL-4-secreting T cells were distinct from conventional T_H2 cells based on phenotype, location and function. Thus, our data are consistent with a model by which IL-4 competency is first generated by interactions with antigen-bearing DCs in the T cell zones³⁷. Upon activation these IL-4 competent cells move to the follicular border and, if they encounter their cognate antigen and ICOS-ligand presented by B cells, they can help in early antibody production or subsequently enter the B cell follicles and participate in the GC reaction. IL-4 competent cells that fail to encounter antigen will leave the lymph node and become canonical T_H2 cells in nonlymphoid tissues. Despite their functional differences, the similar cytokine secretion patterns of T_{FH} cells and peripheral T_H effector cells may explain how humoral and cell-mediated immune responses become coordinated³⁸. Thus, cytokine secretion is segregated to distinct tissues in order to activate different target cells — B cells for T_{FH} cells and innate effector cells for T_H2 cells — in a manner linked with functional differentiation by CD4⁺ T cells as they move into their respective effector sites.

Interestingly, our results with dual IL-4- and IFN- γ -reporter mice suggest that cytokines from T_{FH} cells mediate their effects locally in the germinal center, and not globally in a bystander manner, a concept observed in other T cell systems^{39, 40}. Although competition for rare GC T cells has been suggested as a means to contribute to selection of the highest

affinity B cells, direct evidence for this concept has been absent 3. Despite our data showing that the machinery for isotype-switching and SHM are specifically increased among cytokine-producing conjugates, it is difficult to know exactly when and where affinity maturation and B cell selection actually occur. Our isolation of B cells in conjugates that lacked high-affinity antibody mutations associated with NP-binding, as well as cells that used non-canonical but related heavy chain genes, suggests that competition of GC B cells for IL-4 and IFN- γ from rare T_{FH} cells may allow low-affinity B cells to continue to undergo further rounds of selection within the GC. The process would continue until these GC B cells either acquire a BCR with sufficient affinity for antigen to exit the GC as a plasma cell or memory B cell 41, 42 or die due to insufficient binding required to sustain viability. Although a role for GC T_{FH} cells is clear, it is also likely that IL-4 from T_{FH} cells is playing a role in the early plasma cell response as non-canonical clones are highly enriched in parafollicular foci and are recruited to early GCs 43, 44. Thus, in our model, antigen remains implicit for selection of high-affinity clones, but competition for cytokines allows for the persistence of certain low-affinity clones that would otherwise not be selected.

The need for specific cytokines in the process of affinity maturation was evident from the studies using IL-4-deficient mice (KN2/KN2), in which conjugates formed in the germinal centers but there was a failure to generate high-affinity antigen-specific IgG1 antibodies. The effect of IL-4 on affinity maturation works at some level through increased expression of AID and CD40 ligation, although IL-4 is likely to play additional roles during the GC response 45, 46. Competition for IL-4, a known B cell growth factor, may enhance survival of certain clones and affect B cell clonal diversity throughout the response 43, 44. Of note, IFN- γ -expressing B-T conjugates were also enriched for selection machinery despite the absence of detectable IL-4 expression, confirming that IL-4-independent pathways also exist for affinity maturation.

Although we have not formally accomplished cell-fate tracking experiments, our data are most consistent with the activation of shared cytokine loci before helper T cells migrate into follicles or exit to the periphery to continue their maturation to T_{FH} or T_H subsets. Such a model ensures the pairing of antibody isotype with peripheral cell functions as noted above. Although our model provides a conceptual framework in which to view the role of T_{FH} cell help and cytokines in antibody maturation, definitive proof awaits the ability to track individual B cells *in vivo*. Recent advances in two-photon imaging suggest this may soon be possible and provide the means to assess the dynamic nature of interactions between cytokine-competent T_{FH} cells and B cells in the follicles and GCs 9, 10. Further understanding of the mechanisms by which B-T_{FH} conjugate formation and cytokine secretion regulate cell-fate decisions in the germinal center will be important in optimizing vaccine strategies for eliciting high-affinity antibodies, intervening therapeutically in autoimmune and inflammatory diseases, and in understanding peripheral T and B cell lymphomas that may arise directly or indirectly from chronically activated T_{FH} cells 47, 48

Methods

Mice

Dual IL-4 reporter mice (4get × KN2 mice) have been described¹⁸. In brief, 4get mice were generated by introducing an IRES-eGFP construct after the stop codon of IL-4 by homologous recombination, which leads to transcription of a bicistronic IL-4-IRES-eGFP mRNA and translation of both IL-4 and eGFP from the same mRNA. This allows analysis of IL-4-competent cells *in vivo* by detection of GFP expression without the need for restimulation. KN2 mice were generated by introducing a human CD2 cDNA at the start site of the *il4* gene. After appropriate stimulation, IL-4 secretion becomes marked by the appearance of huCD2 on the cell surface¹⁸. 'Great' (IFN- γ reporter with endogenous polyA tail) mice were generated by introducing an IRES-eYFP construct after the stop codon of the *ifng* gene by homologous recombination. The bicistronic IFN- γ -IRES-eYFP mRNA is under the control of the endogenous *ifng* 3'UTR and polyA tail. Combined IL-4 and IL-13-deficient mice were obtained from A.N. McKenzie (Trinity College, Dublin, Ireland). Mice were maintained in the UCSF specific pathogen-free animal facility in accordance with institutional guidelines.

Infections and immunizations

L. major strain WHOM/IR/-/173 was prepared and injected as $0.5-1 \times 10^6$ metacyclic promastigotes in the hind footpad of mice as described²⁹. *N. brasiliensis* was prepared as described⁴⁹. Mice were immunized with 50 μ g NP-conjugated chicken ovalbumin protein (OVA -NP(15)) (Biosearch Technologies) emulsified in Alum Imject (Pierce) subcutaneously in the footpad or rear flank.

Tissue immunohistochemistry

For detection of eGFP and YFP, the signal was amplified using tyramide amplification on PFA fixed tissue and huCD2 was detected on acetone-dehydrated slides after incubation with biotinylated anti-human CD2 (RPA-2.10, eBioscience). GFP and YFP were detected using rabbit anti-GFP polyclonal antibody (Ab 6556, Novus Biologicals) followed by biotinylated donkey anti-rabbit F(ab')₂ (Jackson ImmunoResearch). In brief, lymph nodes were isolated at indicated times and either frozen directly in O.C.T. embedding compound (Sakura Finetek U.S.A., Inc.) or after 2 h incubation in 1–4% paraformaldehyde (PFA) followed by 30% sucrose. 6–8 μ m sections were cut using a Leica CM 3050S cryomicrotome (Leica Microsystems Inc.). Sections were treated with FITC-tyramide from the TSATM-fluorescein kit according to manufacturer's instructions (Perkin Elmer). Multiple biotinylated antibodies could be detected on the same slide by repeated quenching and blocking of peroxidase and biotin followed by another round of tyramide-Alexafluor 555 (Invitrogen), tyramide-Cy5 or tyramide-biotin (Perkin Elmer) amplification. Other biotinylated antibodies or reagents used were anti-IgD, CD23 (B3B4, BD Pharmingen), or PNA (Vector Labs). Biotinylated donkey-anti-rabbit secondary reagents were used to detect polyclonal rabbit anti-BCL-6 (Abcam). Nuclei were counterstained with 4', 6-diamidino-2'-phenylindole dihydrochloride (DAPI; Roche) in PBS prior to mounting the coverslip. Digital images in the FITC, Cy3 and Cy5 channels were collected using a Nikon Eclipse E800 fluorescence microscope equipped with SimplePCI software (Compix Inc.). Images

were converted to RGB, colored and overlaid using Adobe Photoshop CS2 software (Adobe systems Inc.). In some cases, whole lymph nodes were imaged and collaged using Photoshop.

Flow cytometric analysis of eGFP⁺ and huCD2⁺ cells in draining lymph nodes

Popliteal lymph nodes were isolated from untreated mice or mice infected with *L. major* or immunized with OVA-NP(15). Single-cell suspensions were prepared and labeled with antibodies as listed: GFP⁺ cells were analyzed for expression of huCD2, (555, PE or APC- α -CD2, Caltag), CD4 (RM4-5, Alexa-APC-750- α -CD4, Caltag), CD19 (1D3, PerCP-Cy5.5 or APC- α -CD19, BD-Pharmingen), ICOS (D10.G4.1, PE- α -CD278, Biolegend) and B220 (RA3-6B2, PerCP-Cy5.5 or APC- α -CD45R, BD-Pharmingen and Caltag, respectively), as indicated. Samples were analyzed on a LSR-II (BD Biosciences). Where designated, a dump channel of PerCP-Cy5.5-labeled CD8 α (5H10, BD-pharmingen) and CD11b (M1/70, BD-pharmingen) was used to reduce non-specific staining. Live lymphocytes were gated by DAPI exclusion, size and granularity based on forward- and side-scatter.

Flow cytometric analysis of NP-specific B cells in draining lymph nodes

B cell-T cell doublets and cells for adoptive transfer were sorted using a Moflo cell sorter (Dako Cytomation). Conjugates were dissociated using 2 mM EDTA and vigorous vortexing. Popliteal lymph nodes were isolated from treated and untreated mice and single-cell suspensions were labeled with the following antibodies: B220 (RA3-6B2, Alexa-APC-750- α -CD45R, Caltag), IgD (11-26, PE- α -IgD, Southern Biotech; AMS 9.1, biotin- α -IgD^a, BD-Pharmingen), IgG1 (RMG1-1, biotin- α -IgG1, Biolegend), CD38 (90, FITC- α -CD38, BD-Pharmingen), GL7 (GL7, FITC- α -GL7, BD-Pharmingen), FAS ((Jo2, PE- α -CD95, BD-Pharmingen). NP-specific B cells were labeled with NP conjugated to APC as described 50. Live cells were gated by DAPI exclusion and CD4⁺ (RM4-5, Pacific Blue/Alexa405- α -CD4, Biolegend), CD8⁺ (53-6.7, Pacific Blue- α -CD8, Biolegend) and F4/80⁺ (BM8, Pacific Blue- α -F4/80, eBioscience) cells were included in the DAPI dump channel. Lymphocytes were gated on size and granularity based on forward- and side-scatter.

Real-time RT-PCR

Cells were isolated from mediastinal lymph nodes and lungs of *N. brasiliensis*-infected mice and viable GFP⁺ or GFP⁺huCD2⁺ CD4⁺ T cells were sorted based on DAPI⁻, CD4⁺, CD19⁻, CD8⁻ staining. Cells were lysed and reverse transcribed using Cells Direct cDNA synthesis kit (Invitrogen). Transcripts were quantified using platinum SYBR green incorporation on an Opticon-2 real-time system (Biorad) and plotted relative to expression of HPRT. Primers listed in Supplementary Table 1 online.

Semi-quantitative RT-PCR of switch transcripts from B-T cell conjugates

Draining popliteal lymph nodes were isolated from day 14 *L. major*-infected mice and B-T cell conjugates were sorted based on expression of CD4⁺, CD19⁺, B220⁺, F4/80⁻, and CD8⁻ staining. RNA was isolated and cDNA prepared as described 27. In brief, total RNA was extracted from sorted B-T conjugates and B cell singlets from the designated mice, converted to cDNA, and then normalized by the initial cell numbers to achieve a final

volume for each cDNA sample for use in the RT reaction. A 3-fold serial dilution was then performed on the individual normalized cDNA followed by semi-quantitative PCR. The Pax5 transcript (of B cell origin) level was used to validate both the normalization of cDNA concentration as well as the titration series. PCR for germline and post-switch Ig products was performed as described using 30 to 40 cycles of PCR 27. Conjugates from KN2 \times 4get mice were separated based on GFP⁺ or GFP⁺, huCD2⁺ expression. Conjugates from KN2 \times great mice were separated based on YFP⁺ or huCD2⁺ expression. Primers listed in Supplementary Table 2 online.

Somatic hypermutation

CD4⁻, CD8⁻, CD19⁺, GFP⁻, NP⁺ singlets and CD4⁺, CD8⁻, CD19⁺, CD8⁻ GFP⁺ B-T conjugates were sorted on day 14 post- OVA-NP(15) alum immunization of C57BL/6 4get mice. Genomic DNA was isolated (Puregen genomic DNA kit) and V_H186.2 and J_H4 intronic regions were amplified by nested PCR with Fusion Taq (Finnzyme) 33 and subcloned using Zero Blunt TOPO PCR cloning kit (Invitrogen). Individual clones were selected for sequencing. Two μ l of genomic DNA (equivalent to 1000 cells) were used in initial rounds of nested PCR reactions to amplify the J_H4 intron and V_H186.2 segments.

J_H4 intron primers: 1st round, 5'-GGAATTCGCCTGACATCTGAGGACTCTGC-3' and 5'-CTGGACTTTCGGTTTGGTG-3' for 12 cycles (98 °C for 10 sec, 66 °C for 30 sec, 72 °C 1.5 min), 2nd round, 5'-GGTCAAGGAACCTCAGTCA-3' and 5'-TCTCTAGACAGCAACTAC-3' for 32 cycles (98 °C for 10 sec, 56 °C for 30 sec, 72 °C 30 sec). V_H186.2 primers: 1st round, 5'-ACACAGGACCTCACCATG-3' and 5'-TCACAAGAGTCCGATAGACC-3' for 12 cycles (98 °C for 10 sec, 60 °C for 30 sec, 72 °C 1.5 min), 2nd round, 5'-GGGTGACAATGACATCCA-3' and 5'-GAGGAGACTGTGAGAGTGGTGCC-3' for 32 cycles (98 °C for 10 sec, 62 °C for 30 sec, 72 °C 30 sec).

Enzyme-Linked Immunosorbent Assay (ELISA)

To detect NP-specific antibodies in serum of immunized mice, 96-well plates were coated with NP(23)-BSA or NP(3)-BSA (Biosearch) and incubated with serial 5-fold dilutions of serum. IgG1 NP-specific antibodies were detected by incubation with biotinylated anti-mouse IgG1 followed by streptavidin-HRP and o-phenylenediamine (OPD). Affinity maturation was determined as described 14. Briefly, the concentration of serum anti-NP antibodies bound to NP(3)-BSA was divided by the concentration anti-NP antibodies bound to NP(23)-BSA. As the affinity of the antibodies increase, the ratio approaches one. The concentrations of anti-NP IgG1 were determined by comparison to standard curves generated using IgG1 from the anti-NP, IgG1 clone H33L γ 1/ λ 1 (kindly provided by G. Kelsoe, Duke University).

Enzyme-Linked Immunospot (ELISPOT)

To detect NP-specific antibody-secreting cells (ASC), single-cell suspensions were cultured in plates coated with NP(23)-BSA. NP-specific IgG1 was visualized with biotinylated anti-mouse IgG1 followed by streptavidin-alkaline phosphatase and 5-bromo-4-chloro-3-indolylphosphate *p*-toluidine salt (BCIP, Sigma) diluted in alkaline buffer containing 0.6%

agarose. For detection of IL-21-secreting cells, CD4⁺, CD8⁻, F4/80⁻, B220⁻ cells were isolated from the lungs and lymph nodes of *N. brasiliensis*-infected mice 10–12 days post-infection and sorted based on GFP expression. CD4⁺ T cells were plated at serial 2-fold dilutions into Millipore MultiScreen HTS 96-well plates coated with goat polyclonal anti-IL-21 capture antibody (AF594, R&D Systems). Cells were harvested after 48 h at 37° C with or without PMA and ionomycin treatment and IL-21 was detected using biotinylated goat polyclonal anti-IL-21 (BAF594, R&D Systems) followed by streptavidin-alkaline phosphatase and BCIP/NBT (Vector Labs).

Supplementary Material

Refer to Web version on PubMed Central for supplementary material.

Acknowledgements

The authors thank G. Kelsoe, M. Nussenzweig, K. McBride, and A. N. McKenzie for reagents and helpful suggestions, J. Cyster (UCSF), A. DeFranco (UCSF), and C. Allen (UCSF) for expert review and comments, and N. Flores, L. Stowring and C. McArthur for technical expertise. This work was supported by AI026918 and AI077439 from the National Institutes of Allergy and Infectious Diseases, the Howard Hughes Medical Institute and the Sandler Asthma Basic Research Center at UCSF. R. L. R. is a Juvenile Diabetes Research Foundation-Irvington Institute Fellow.

References

1. MacLennan IC. Germinal centers. *Annu Rev Immunol.* 1994; 12:117–139. [PubMed: 8011279]
2. Kelsoe G. Life and death in germinal centers (redux). *Immunity.* 1996; 4:107–111. [PubMed: 8624801]
3. Allen CD, Okada T, Cyster JG. Germinal-center organization and cellular dynamics. *Immunity.* 2007; 27:190–202. [PubMed: 17723214]
4. Fang Y, Xu C, Fu YX, Holers VM, Molina H. Expression of complement receptors 1 and 2 on follicular dendritic cells is necessary for the generation of a strong antigen-specific IgG response. *J Immunol.* 1998; 160:5273–5279. [PubMed: 9605124]
5. Hannum LG, Haberman AM, Anderson SM, Shlomchik MJ. Germinal center initiation, variable gene region hypermutation, and mutant B cell selection without detectable immune complexes on follicular dendritic cells. *J Exp Med.* 2000; 192:931–942. [PubMed: 11015435]
6. Huntington ND, et al. CD45 links the B cell receptor with cell survival and is required for the persistence of germinal centers. *Nat Immunol.* 2006; 7:190–198. [PubMed: 16378097]
7. Allen D, Simon T, Sablitzky F, Rajewsky K, Cumano A. Antibody engineering for the analysis of affinity maturation of an anti-hapten response. *The EMBO journal.* 1988; 7:1995–2001. [PubMed: 3138111]
8. Meyer-Hermann ME, Maini PK, Iber D. An analysis of B cell selection mechanisms in germinal centers. *Math Med Biol.* 2006; 23:255–277. [PubMed: 16707510]
9. Allen CD, Okada T, Tang HL, Cyster JG. Imaging of germinal center selection events during affinity maturation. *Science.* 2007; 315:528–531. [PubMed: 17185562]
10. Schwickert TA, et al. In vivo imaging of germinal centres reveals a dynamic open structure. *Nature.* 2007; 446:83–87. [PubMed: 17268470]
11. King C, Tangye SG, Mackay CR. T Follicular Helper (T(FH)) Cells in Normal and Dysregulated Immune Responses. *Annu Rev Immunol.* 2008
12. Fazilleau N, McHeyzer-Williams LJ, McHeyzer-Williams MG. Local development of effector and memory T helper cells. *Curr Opin Immunol.* 2007; 19:259–267. [PubMed: 17420119]
13. Garside P, et al. Visualization of specific B and T lymphocyte interactions in the lymph node. *Science.* 1998; 281:96–99. [PubMed: 9651253]

14. Takahashi Y, Dutta PR, Cerasoli DM, Kelsoe G. In situ studies of the primary immune response to (4-hydroxy-3-nitrophenyl)acetyl. V. Affinity maturation develops in two stages of clonal selection. *J Exp Med*. 1998; 187:885–895. [PubMed: 9500791]
15. Chtanova T, et al. T follicular helper cells express a distinctive transcriptional profile, reflecting their role as non-Th1/Th2 effector cells that provide help for B cells. *J Immunol*. 2004; 173:68–78. [PubMed: 15210760]
16. Vogelzang A, et al. A fundamental role for interleukin-21 in the generation of T follicular helper cells. *Immunity*. 2008; 29:127–137. [PubMed: 18602282]
17. Nurieva RI, et al. Generation of T follicular helper cells is mediated by interleukin-21 but independent of T helper 1, 2, or 17 cell lineages. *Immunity*. 2008; 29:138–149. [PubMed: 18599325]
18. Mohrs K, Wakil AE, Killeen N, Locksley RM, Mohrs M. A two-step process for cytokine production revealed by IL-4 dual-reporter mice. *Immunity*. 2005; 23:419–429. [PubMed: 16226507]
19. Vinuesa CG, Tangye SG, Moser B, Mackay CR. Follicular B helper T cells in antibody responses and autoimmunity. *Nat Rev Immunol*. 2005; 5:853–865. [PubMed: 16261173]
20. Loke P, et al. Inducible costimulator is required for type 2 antibody isotype switching but not T helper cell type 2 responses in chronic nematode infection. *Proc Natl Acad Sci U S A*. 2005; 102:9872–9877. [PubMed: 15994233]
21. Tafuri A, et al. ICOS is essential for effective T-helper-cell responses. *Nature*. 2001; 409:105–109. [PubMed: 11343123]
22. Dong C, Temann UA, Flavell RA. Cutting edge: critical role of inducible costimulator in germinal center reactions. *J Immunol*. 2001; 166:3659–3662. [PubMed: 11238604]
23. Finkelman FD, et al. Interleukin-4-and interleukin-13-mediated host protection against intestinal nematode parasites. *Immunol Rev*. 2004; 201:139–155. [PubMed: 15361238]
24. Voehringer D, Shinkai K, Locksley RM. Type 2 immunity reflects orchestrated recruitment of cells committed to IL-4 production. *Immunity*. 2004; 20:267–277. [PubMed: 15030771]
25. Okada T, et al. Antigen-engaged B cells undergo chemotaxis toward the T zone and form motile conjugates with helper T cells. *PLoS biology*. 2005; 3:e150. [PubMed: 15857154]
26. Casamayor-Palleja M, Feuillard J, Ball J, Drew M, MacLennan IC. Centrocytes rapidly adopt a memory B cell phenotype on co-culture with autologous germinal centre T cell-enriched preparations. *Int Immunol*. 1996; 8:737–744. [PubMed: 8671662]
27. Muramatsu M, et al. Class switch recombination and hypermutation require activation-induced cytidine deaminase (AID), a potential RNA editing enzyme. *Cell*. 2000; 102:553–563. [PubMed: 11007474]
28. Muramatsu M, et al. Specific expression of activation-induced cytidine deaminase (AID), a novel member of the RNA-editing deaminase family in germinal center B cells. *The Journal of biological chemistry*. 1999; 274:18470–18476. [PubMed: 10373455]
29. Reiner SL, Zheng S, Wang ZE, Stowring L, Locksley RM. Leishmania promastigotes evade interleukin 12 (IL-12) induction by macrophages and stimulate a broad range of cytokines from CD4⁺ T cells during initiation of infection. *J Exp Med*. 1994; 179:447–456. [PubMed: 7905017]
30. Bothwell AL, et al. Heavy chain variable region contribution to the NPb family of antibodies: somatic mutation evident in a gamma 2a variable region. *Cell*. 1981; 24:625–637. [PubMed: 6788376]
31. Rajewsky K, Forster I, Cumano A. Evolutionary and somatic selection of the antibody repertoire in the mouse. *Science*. 1987; 238:1088–1094. [PubMed: 3317826]
32. Jolly CJ, Klix N, Neuberger MS. Rapid methods for the analysis of immunoglobulin gene hypermutation: application to transgenic and gene targeted mice. *Nucleic acids research*. 1997; 25:1913–1919. [PubMed: 9115357]
33. Dorsett Y, et al. MicroRNA-155 suppresses activation-induced cytidine deaminase-mediated Myc-Igh translocation. *Immunity*. 2008; 28:630–638. [PubMed: 18455451]
34. Reiter R, Pfeffer K. Impaired germinal centre formation and humoral immune response in the absence of CD28 and interleukin-4. *Immunology*. 2002; 106:222–228. [PubMed: 12047751]

35. Vajdy M, Kosco-Vilbois MH, Kopf M, Kohler G, Lycke N. Impaired mucosal immune responses in interleukin 4-targeted mice. *J Exp Med.* 1995; 181:41–53. [PubMed: 7807021]
36. Andoh A, Masuda A, Yamakawa M, Kumazawa Y, Kasajima T. Absence of interleukin-4 enhances germinal center reaction in secondary immune response. *Immunology letters.* 2000; 73:35–41. [PubMed: 10963809]
37. Itano AA, Jenkins MK. Antigen presentation to naive CD4 T cells in the lymph node. *Nat Immunol.* 2003; 4:733–739. [PubMed: 12888794]
38. Nimmerjahn F, Ravetch JV. Fcγ receptors: old friends and new family members. *Immunity.* 2006; 24:19–28. [PubMed: 16413920]
39. Reichert P, Reinhardt RL, Ingulli E, Jenkins MK. Cutting edge: in vivo identification of TCR redistribution and polarized IL-2 production by naive CD4 T cells. *J Immunol.* 2001; 166:4278–4281. [PubMed: 11254679]
40. Maldonado RA, Irvine DJ, Schreiber R, Glimcher LH. A role for the immunological synapse in lineage commitment of CD4 lymphocytes. *Nature.* 2004; 431:527–532. [PubMed: 15386021]
41. Phan TG, et al. High affinity germinal center B cells are actively selected into the plasma cell compartment. *J Exp Med.* 2006; 203:2419–2424. [PubMed: 17030950]
42. Tarlinton DM. Evolution in miniature: selection, survival and distribution of antigen reactive cells in the germinal centre. *Immunol Cell Biol.* 2008; 86:133–138. [PubMed: 18180800]
43. Jacob J, Przylepa J, Miller C, Kelsoe G. In situ studies of the primary immune response to (4-hydroxy-3-nitrophenyl)acetyl. III. The kinetics of V region mutation and selection in germinal center B cells. *J Exp Med.* 1993; 178:1293–1307. [PubMed: 8376935]
44. Dal Porto JM, Haberman AM, Shlomchik MJ, Kelsoe G. Antigen drives very low affinity B cells to become plasmacytes and enter germinal centers. *J Immunol.* 1998; 161:5373–5381. [PubMed: 9820511]
45. Zhou C, Saxon A, Zhang K. Human activation-induced cytidine deaminase is induced by IL-4 and negatively regulated by CD45: implication of CD45 as a Janus kinase phosphatase in antibody diversification. *J Immunol.* 2003; 170:1887–1893. [PubMed: 12574355]
46. Dedeoglu F, Horwitz B, Chaudhuri J, Alt FW, Geha RS. Induction of activation-induced cytidine deaminase gene expression by IL-4 and CD40 ligation is dependent on STAT6 and NFκB. *Int Immunol.* 2004; 16:395–404. [PubMed: 14978013]
47. de Leval L, et al. The gene expression profile of nodal peripheral T-cell lymphoma demonstrates a molecular link between angioimmunoblastic T-cell lymphoma (AITL) and follicular helper T (TFH) cells. *Blood.* 2007; 109:4952–4963. [PubMed: 17284527]
48. Zangani MM, et al. Lymphomas can develop from B cells chronically helped by idiotype-specific T cells. *J Exp Med.* 2007; 204:1181–1191. [PubMed: 17485509]
49. Shinkai K, Mohrs M, Locksley RM. Helper T cells regulate type-2 innate immunity in vivo. *Nature.* 2002; 420:825–829. [PubMed: 12490951]
50. Lalor PA, Nossal GJ, Sanderson RD, McHeyzer-Williams MG. Functional and molecular characterization of single, (4-hydroxy-3-nitrophenyl)acetyl (NP)-specific, IgG1+ B cells from antibody-secreting and memory B cell pathways in the C57BL/6 immune response to NP. *Eur J Immunol.* 1992; 22:3001–3011. [PubMed: 1425924]

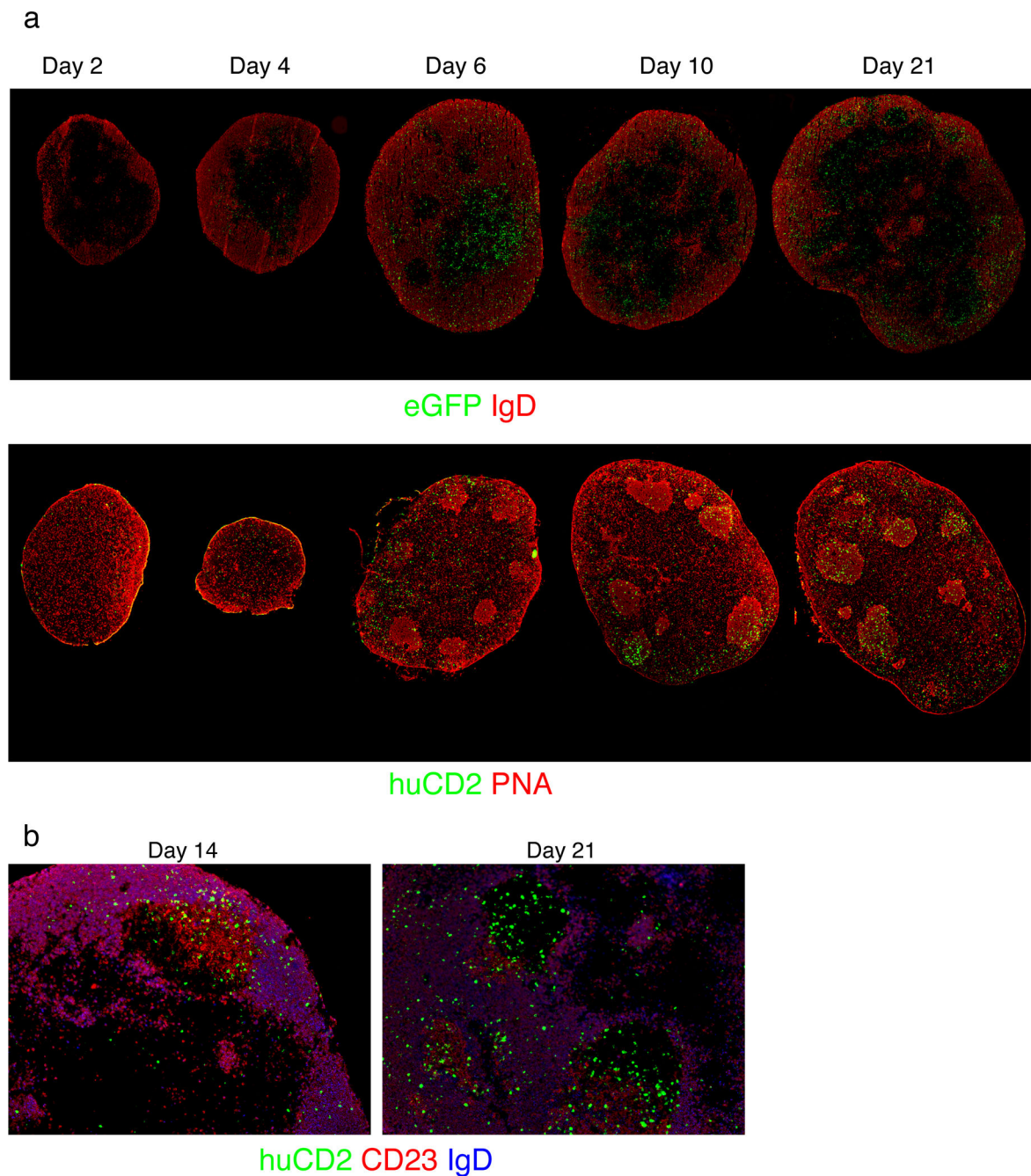


Figure 1. Kinetics and identification of IL-4-producing cells in the draining lymph nodes after *L. major* infection

(a) Sections of the draining popliteal lymph nodes from KN2 × 4get dual reporter mice infected with *L. major* were stained for GFP (green, IL-4-competent cells), and IgD (red, B cell follicles) (top) and human CD2 (green, IL-4-secreting cells) and PNA (red, germinal centers) (bottom) at the indicated times post-infection. Individual 40x images were merged to form the composite picture of the lymph node. In bottom panel green staining was increased by 5 pixels. Time points are representative of at least two independent experiments (n = 2–4 lymph nodes).

(b) The expression of human CD2 (IL-4-secreting cells) was analyzed *in situ* on sections from the draining lymph nodes 14 and 21 days after *L. major* infection. 100x images from slides stained for human CD2 (green), CD23 (red, follicular dendritic cell), and IgD (blue, B cell follicles). GC light and dark zones were identified by the presence and absence of CD23 staining, respectively. Sections are representative of two lymph nodes per time point.

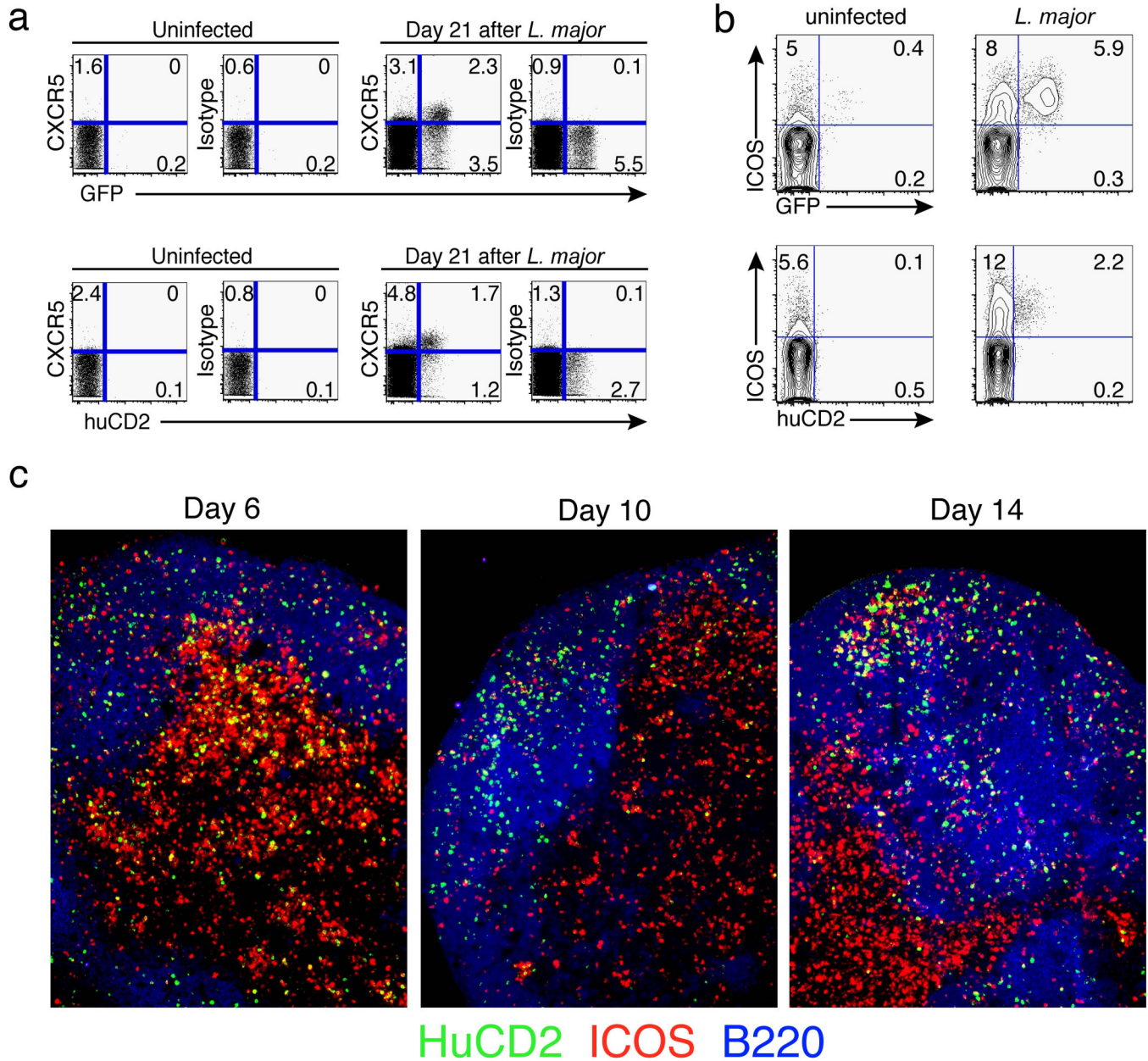


Figure 2. IL-4 producing cells in the lymph node coexpress ICOS, CXCR5, and human CD2⁺ in KN2 × 4get mice after *L. major* infection

(a) Flow cytometry of draining popliteal lymph node cells from KN2 × 4get dual reporter mice infected with *L. major* 21 days previously. Plots represent CD4⁺, DAPI⁻, B220⁻, CD8⁻ lymphocytes. The numbers in each quadrant represent the percent of cells expressing CXCR5 plotted against GFP or huCD2. Plots are representative of at least two independent experiments (n = 5–7 mice).

(b) Flow cytometry of CD4⁺ T cells from *L. major*-infected lymph nodes. Numbers represent the percentage of CD4⁺ T cells expressing ICOS and GFP or ICOS and huCD2

among total CD4⁺ T cells. Plots are representative of 10 mice from 4 independent experiments.

(c) KN2 × 4get mice were infected with 0.5×10^6 *L. major* promastigotes and the draining lymph nodes were examined at the indicated times. Popliteal lymph nodes were sectioned and stained for human CD2 (green), ICOS (red), B220 (blue).

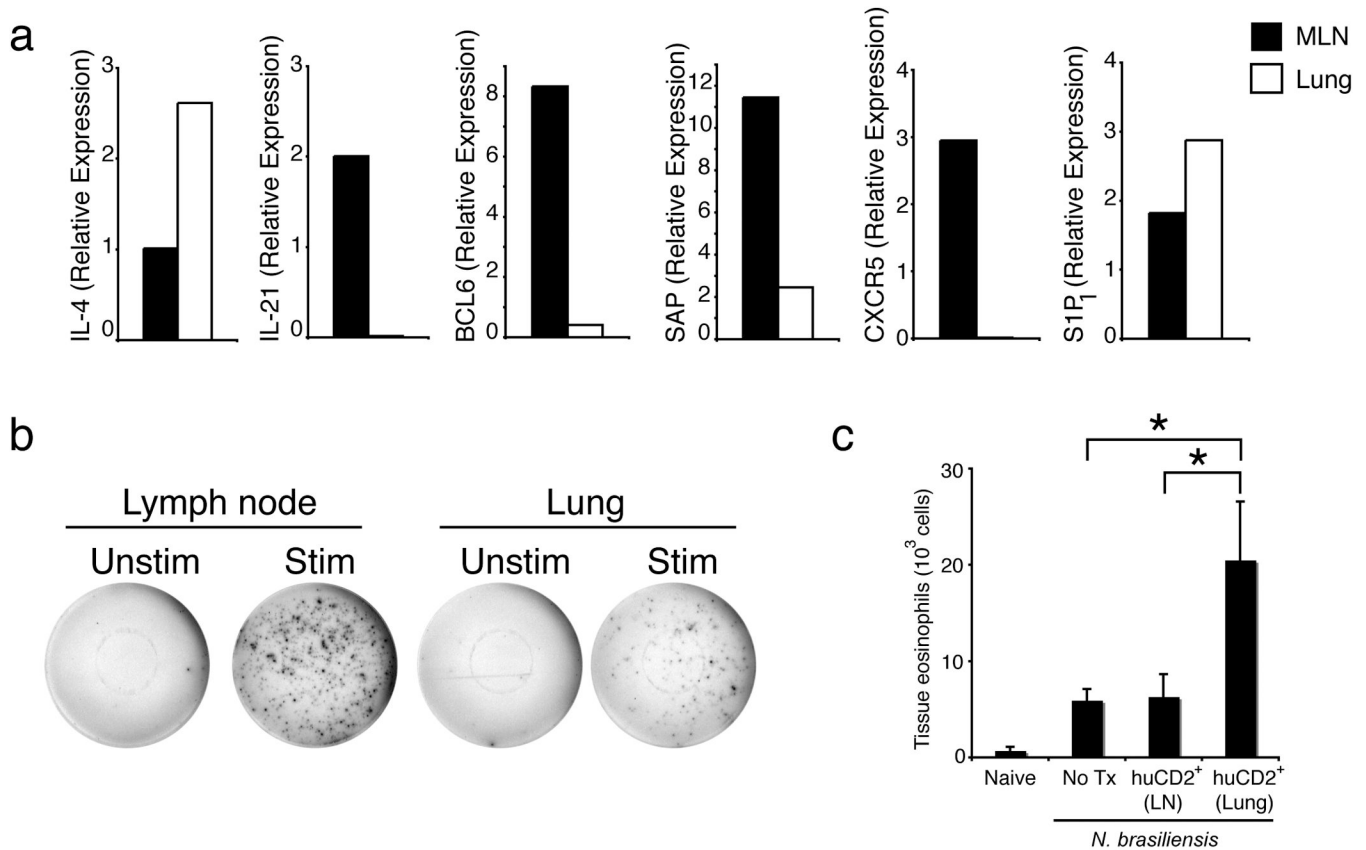


Figure 3. IL-4-producing CD4 T cells in lymph nodes are T_{H1} cells and are functionally distinct from canonical T_{H2} cells

(a) Relative expression of mRNA transcripts plotted against housekeeping gene HPRT for the indicated genes from CD4⁺ T cells isolated from the lymph nodes and lungs of mice infected with *N. brasiliensis* 9 days previously. Data are representative of at least two independent experiments.

(b) ELISPOT assay for IL-21-secreting cells from tissues of mice infected with *N. brasiliensis* 10 days previously. GFP⁺, CD4⁺ T cells were isolated and sorted from the indicated organs and cultured in the presence or absence of PMA plus ionomycin. Data are representative of at least 3 independent experiments.

(c) Eosinophil recruitment into the lung 10 days post-*N. brasiliensis* infection of combined IL-4 and 13-deficient mice adoptively transferred with 50,000 GFP⁺, huCD2⁺, CD4⁺ T cells from the lymph node (huCD2⁺ LN) or lung (huCD2⁺ Lung) compared to infected mice that received no T cell transfer (No Tx) or uninfected naïve (Naïve) combined IL-4 and 13-deficient controls. Total Siglec-F^{hi} tissue eosinophils ± S.E.M. (*n* = 5–9 mice per group combined from 3 independent experiments). * (*P* < 0.01)

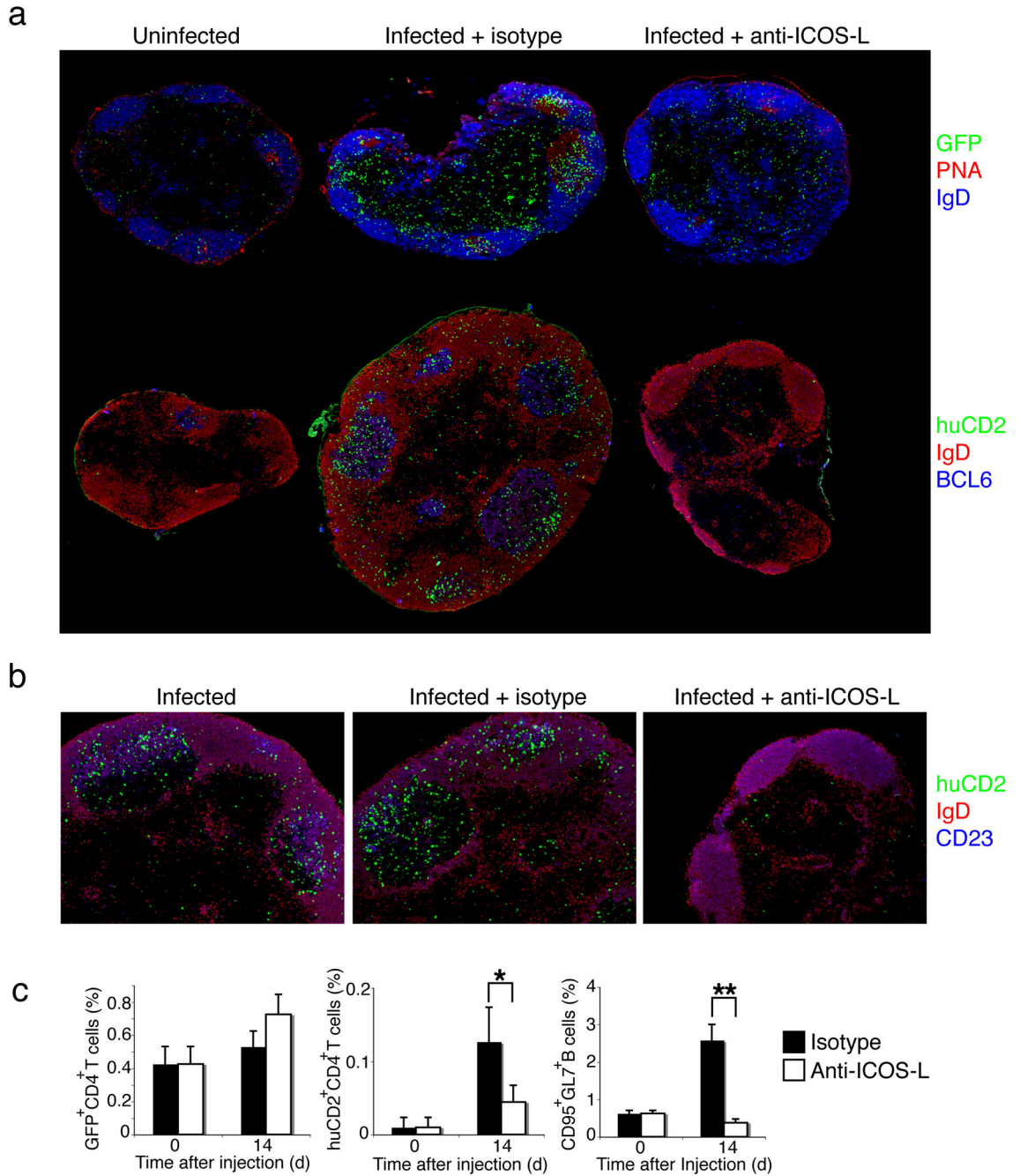


Figure 4. ICOS regulates IL-4 production by follicular T helper cells

KN2 × 4get dual reporter mice were infected with *L. major* and injected every other day with 100 μg of anti-ICOS-L antibody or isotype control. The draining popliteal lymph nodes were isolated 14 days after infection.

(a) Sections from draining popliteal lymph nodes were stained as indicated. Top, anti-GFP (green, IL-4-competent cells), PNA (red, GC) and anti-IgD (blue, B cell follicles). Bottom, anti-human CD2 (green, IL-4-secreting cells), anti-IgD (red, B cell follicles) and anti-BCL6 (blue, GC). Individual 40x images were merged to form the composite picture of the whole

lymph node. Images are representative of lymph nodes from at least two independent experiments (n = 2–4 mice).

(b) 100x images taken from popliteal lymph nodes of *L. major*-infected mice stained with anti-human CD2 (green), anti-IgD (red, B cell follicles) and anti-CD23 (blue, follicular DC).

(c) Graphs represent the percentage of GFP or huCD2-expressing CD4⁺ T cells or CD95⁺, GL7⁺ germinal center B cells among total lymphocytes in draining lymph nodes of OVA-NP(15)-challenged mice after treatment with anti-ICOS-L (white bars) or isotype control (black bars). *($P < 0.01$); **($P < 0.001$). Data representative of at least two independent experiments (n = 4 mice).

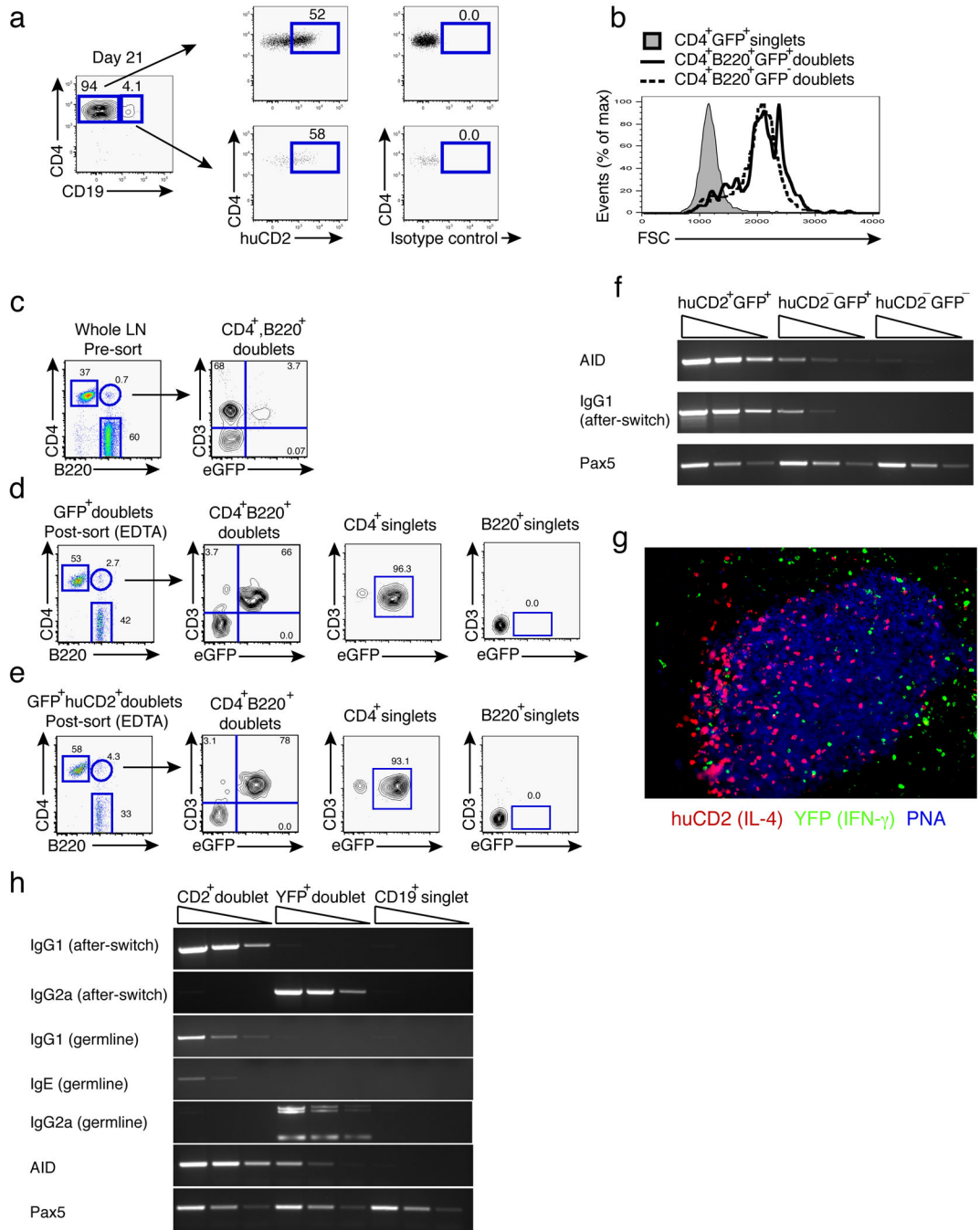


Figure 5. B–T conjugates regulate immunoglobulin class-switching

(a) Mice were infected with *L. major* and draining lymph nodes were harvested 21 days after infection. HuCD2 (IL-4 secretion) expression on GFP⁺ CD4⁺ T cells or B–T cell conjugates gated in leftmost panel are indicated by arrows in the four panels of which the first panels denote staining with anti-human CD2 and the right panels denote staining with an isotype control antibody. Plots are representative of at least six experiments (n = 2–4 mice per experiment).

- (b)** Size as marked by forward-size scatter of GFP⁺, CD4⁺, B220⁺ co-expressing conjugates compared to GFP⁺ singlet or GFP⁻ doublet cells in the draining lymph node of KN2 × 4get mice.
- (c)** Gating scheme of CD4⁺ T cell and B cell doublets in the draining lymph node of *L. major*-infected KN2 × 4get mice prior to sorting. All GFP⁺, CD4⁺, B220⁺ cells express the T cell receptor-associated CD3 marker.
- (d)** GFP⁺, CD4⁺, B220⁺ doublets sorted from **(a)** were treated with 2 mM EDTA post-sort and reanalyzed by flow cytometry. Plots are representative of combined lymph nodes from at least two independent experiments (n = 2–3 mice).
- (e)** huCD2⁺, CD4⁺, B220⁺ doublets sorted from **(a)** were treated with 2 mM EDTA and reanalyzed by flow cytometry. Plots are representative of combined lymph nodes from at least two independent experiments (n = 2–3 mice).
- (f)** B–T cell conjugates from KN2 × 4get dual reporter mice were sorted 14 days after *L. major* infection from draining popliteal lymph nodes and semi-quantitative RT-PCR was performed for expression of AID and IgG1-post-switch transcripts. cDNA from GFP⁺; GFP⁺, huCD2⁺; or GFP⁻, huCD2⁻ CD4⁺ B–T cell conjugates was normalized to Pax5 expression to ensure equivalent amounts of B cell cDNA was added per reaction. Gels are representative of at least two independent experiments with cDNA at 3 serial dilutions.
- (g)** 200x image from section of the draining popliteal lymph node from KN2 × great mice 14 days after *L. major* infection. huCD2 (Red, IL-4-secretion), YFP (green, IFN- γ -competence), PNA (blue, germinal centers). Image is representative of 6 lymph nodes from at least two independent experiments.
- (h)** B–T cell conjugates from KN2 × great dual reporter mice were sorted 14 days after *L. major* infection from draining popliteal lymph nodes and semi-quantitative RT-PCR was performed for expression of AID, IgG1 and IgG2a switch and germline transcripts. cDNA from YFP⁺ or huCD2⁺ CD4⁺, CD19⁺ B–T cell conjugates or GFP⁻, huCD2⁻, CD4⁻, CD19⁺ singlets was normalized to Pax5 expression to ensure equivalent amounts of B cell cDNA was added per reaction and gels were loaded with 3 serial dilutions of cDNA. Gel is representative of at least two independent experiments with cDNA used at three serial dilutions.

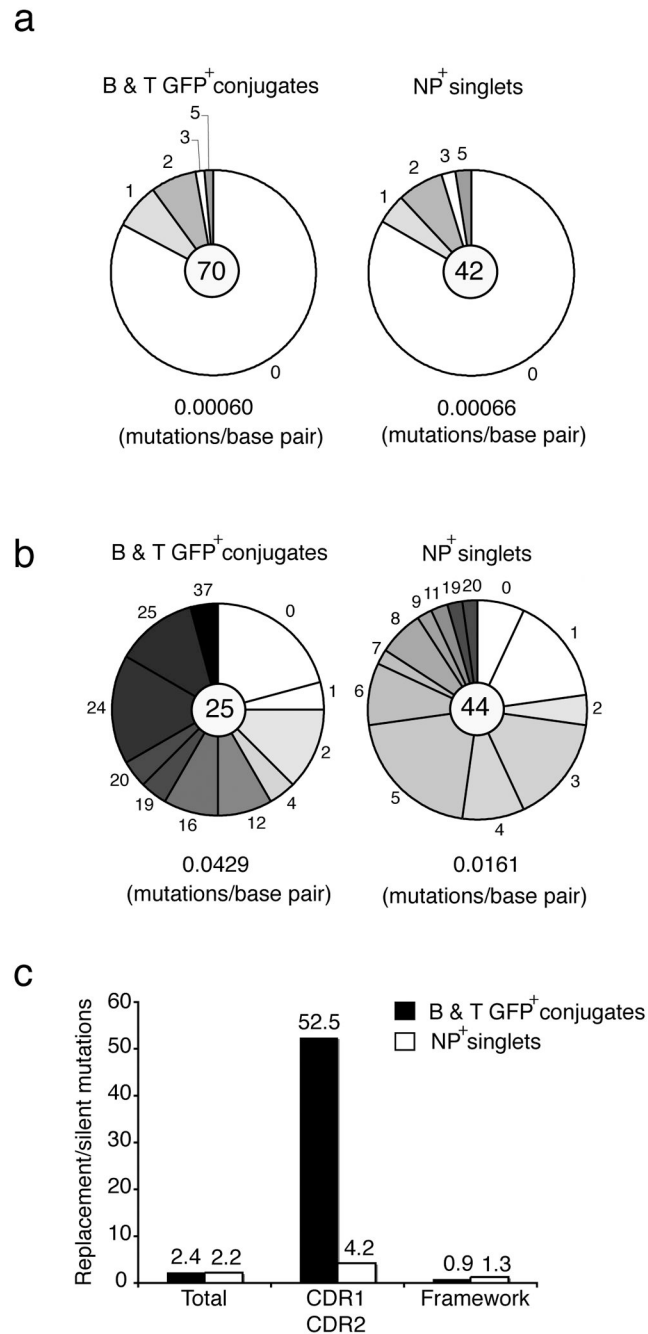


Figure 6. Somatic hypermutation on day 14 in J_H4 intron and V_H 186.2 region among B–T conjugates and NP-specific B cells after OVA-NP(15) alum injection

(a) Analysis of J_H4 introns cloned from B–T conjugates and NP⁺ B cell singlets. The pie charts represent the number of unique clones (70 clones for B–T conjugates; 42 clones for NP-singlets) with nucleotide mutations in the J_H4 region. Pie segments are proportional to the number of sequences with the marked number of nucleotide changes. The mutation frequency is indicated below the pie chart and represents the number of mutations per base pair. Data compiled from two independent experiments.

(b) Analysis of V_H186.2 heavy chains cloned from GFP⁺ B–T conjugates and NP⁺ B cell singlets 14 days post-injection of OVA-NP. The pie charts represent the number of unique clones (25 clones for B–T conjugates; 44 clones for NP-singlets) sequenced for nucleotide mutations in the V-region. Pie segments are proportional to the number of sequences with the marked number of nucleotide changes. The mutation frequency is indicated below the pie chart and represents the number of mutations per base pair. Data compiled from two independent experiments.

(c) The graph represents the ratio of amino acid replacement mutations to silent mutations within the framework and complementarity-determining regions compared to the canonical V_H186.2 gene in GFP⁺ B–T conjugates (filled bars) and NP-specific B cells (open bars). Data compiled from two independent experiments.

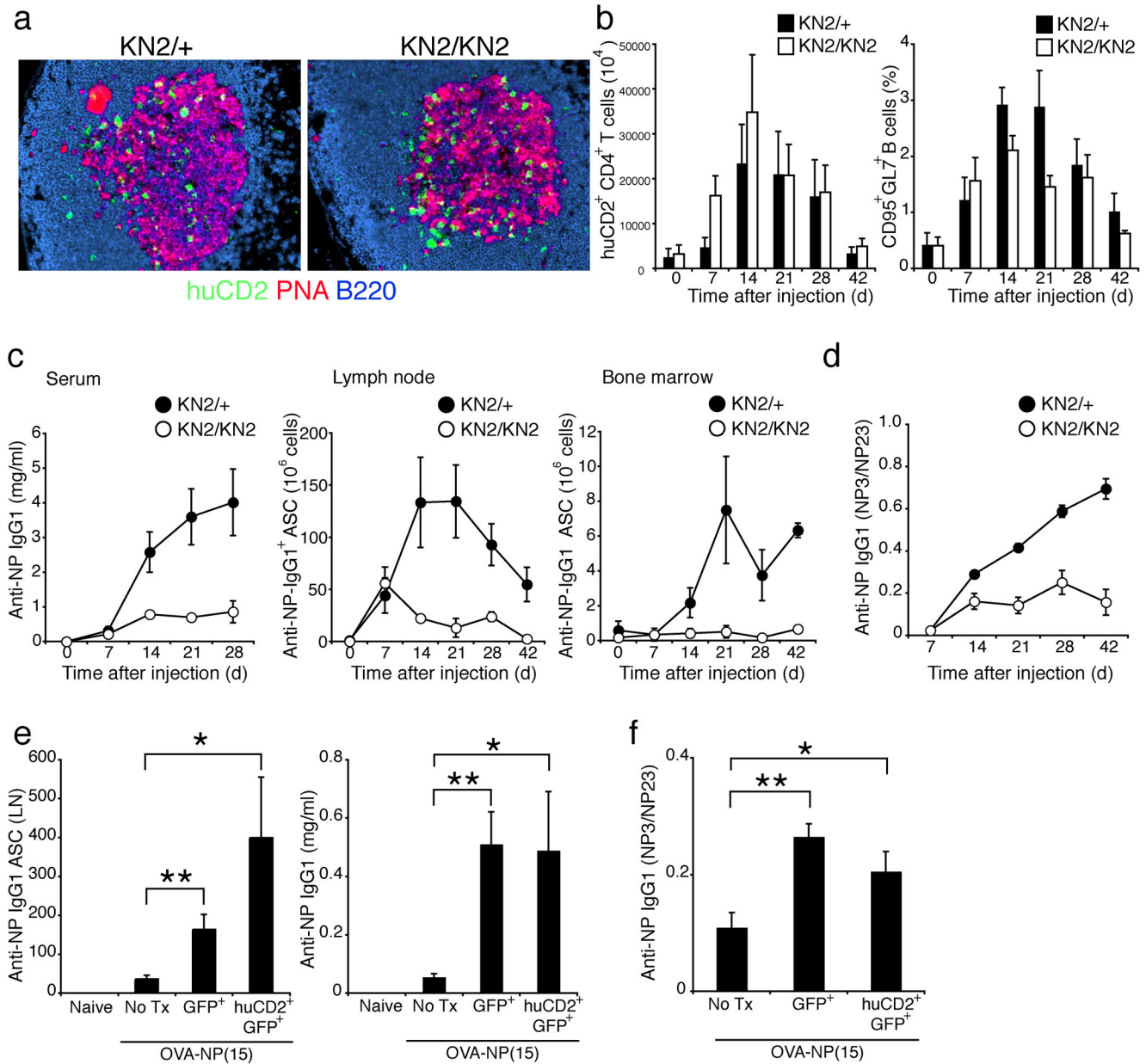


Figure 7. Role of IL-4-producing T_{FH} cells in plasma cell generation and affinity maturation

(a) Mice homozygous or heterozygous for the KN2 knock-in allele were immunized with OVA-NP(15) precipitated in alum. 100x images of germinal centers in KN2/+ (IL-4-sufficient) and KN2/KN2 (IL-4-deficient) mice 14 days after immunization. Sections were stained with anti-human CD2 (green, IL-4-secreting cells), anti-PNA (red, GC) and anti-B220 (blue, B cell follicles).

(b) The graphs represent the total number of huCD2⁺, CD4⁺ T cells and germinal center B cells ± S.E.M. (*n* = 6 mice per group combined from two independent experiments) at each time after OVA-NP(15) injection in KN2/+ (black bars) and KN2/KN2 (white bars).

(c) The graphs represent the number of anti-NP IgG1-secreting cells in the draining lymph node and bone marrow and the concentration of NP specific IgG1 antibodies in the serum ±

S.E.M. ($n = 6$ mice per group combined from two independent experiments) of infected KN2/+ (closed circles) and KN2/KN2 (open circles) mice following OVA-NP(15) challenge that are able to bind to BSA-NP(23).

(d) The graph represents affinity maturation of serum anti-NP-specific IgG1 antibodies from KN2/+ mice (closed circles) and KN2/KN2 (open circles) following OVA-NP(15) challenge. Ratio depicts binding of serum IgG1 to BSA-NP(3)/BSA-NP(23) \pm S.E.M. ($n = 6$ mice per group combined from two independent experiments).

(e) CD4⁺, GFP⁺ T cells were isolated from KN2 \times 4get dual reporter mice 14 days after OVA-NP(15) injection and 25,000–50,000 GFP⁺ (GFP⁺) or huCD2⁺ (huCD2⁺, GFP⁺) cells were transferred into combined IL-4 and 13-deficient hosts. Draining lymph nodes and serum were collected on day 14 after OVA-NP(15) challenge. Serum IgG1 antibodies and AFCs from transferred mice were compared to naïve (Naïve) and untransferred (No Tx) combined IL-4 and IL-13 deficient mice. The bars represent the number of anti-NP IgG1-secreting cells and concentration of high-affinity anti-NP-specific IgG1 antibodies in the serum \pm S.E.M. ($n = 6$ mice per group combined from two independent experiments) that are able to bind BSA-NP(3). *($p < 0.05$); **($p < 0.01$)

(f) Serum IgG1 was collected from OVA-NP(15) challenged combined IL-4 and 13-deficient mice. Combined IL-4 and 13-deficient mice were left untransferred (No Tx) or transferred with 25,000–50,000 GFP⁺ (GFP⁺) or huCD2⁺, GFP (huCD2⁺, GFP⁺), CD4⁺ T cells prior to challenge. Affinity maturation was measured as a ratio of serum anti-NP IgG1 antibodies bound to NP(3)-BSA/NP(23) BSA. *($p < 0.05$); **($p < 0.001$)